



# CHORUS

This is the accepted manuscript made available via CHORUS. The article has been published as:

## Explaining the CMS Higgs flavor-violating decay excess

D. Aristizabal Sierra and A. Vicente

Phys. Rev. D **90**, 115004 — Published 3 December 2014

DOI: [10.1103/PhysRevD.90.115004](https://doi.org/10.1103/PhysRevD.90.115004)

# Explaining the CMS Higgs flavor violating decay excess

D. Aristizabal Sierra\* and A. Vicente†

*IFPA, Dep. AGO, Université de Liège, Bat B5, Sart-Tilman B-4000 Liège 1, Belgium*

Direct searches for lepton flavor violating Higgs boson decays in the  $\tau\mu$  channel have been recently reported by the CMS collaboration. The results display a slight excess of signal events with a significance of  $2.5\sigma$ , which translates into a branching ratio of about 1%. By interpreting these findings as a hint for beyond the standard model physics, we show that the Type-III 2HDM is capable of reproducing such signal while at the same time satisfying boundedness from below of the scalar potential, perturbativity, electroweak precision data, measured Higgs standard decay modes and low-energy lepton flavor violating constraints. We have found that the allowed signal strength ranges for the  $b\bar{b}$ ,  $WW^*$  and  $ZZ^*$  standard channels shrink as soon as  $\text{BR}(h \rightarrow \tau\mu) \sim 1\%$  is enforced. Thus, we point out that if the excess persists, improved measurements of these channels may be used to test our Type-III 2HDM scenario.

PACS numbers: 12.60.-i, 12.60.Fr

Keywords: models beyond the standard models, Higgs sector extensions

## I. INTRODUCTION

Since the discovery of the Higgs boson [1, 2] special effort has been made to determine its properties. The motivation for such an effort resides on understanding the mechanism for electroweak symmetry breaking. At present, several aspects of the Higgs boson are to some extent well known, in particular those related with some of its expected “standard” decay modes, namely:  $WW^*$ ,  $ZZ^*$ ,  $\gamma\gamma$ ,  $b\bar{b}$  and  $\tau\bar{\tau}$ . Currently, measurements of these decay modes have shown compatibility with the standard model (SM) expectations, although with large associated uncertainties [3]. Indeed, it is due to these large uncertainties that there is still room for nonstandard decay properties, something that has encouraged such searches at the LHC as well. Searches for invisible Higgs decays have been published in [4, 5], while direct searches for lepton flavor violating Higgs decays ( $h \rightarrow \tau\mu$ ) have been recently reported by the CMS collaboration in [6]. In this letter we focus on the latter, for which the CMS collaboration, using the 2012 dataset taken at  $\sqrt{s} = 8$  TeV with an integrated luminosity of  $19.7 \text{ fb}^{-1}$ , has found a  $2.5\sigma$  excess in the  $h \rightarrow \tau\mu$  channel, which translates into  $\text{BR}(h \rightarrow \tau\mu) = (0.89_{-0.37}^{+0.40})\%$ .

Indirect bounds on Higgs lepton flavor violating decay modes arise from low-energy data. Muon and tau rare decays (e.g.  $\mu \rightarrow e\gamma$ ,  $\mu \rightarrow 3e$ ,  $\tau \rightarrow e\gamma$  and  $\tau \rightarrow 3\mu$ )—induced by Higgs lepton flavor breaking couplings—place upper bounds on the Higgs flavor violating modes:  $h \rightarrow \tau\mu$ ,  $h \rightarrow \tau e$ ,  $h \rightarrow \mu e$ . Since muon decays have the most tight limits, it is for the  $\mu e$  mode for which consistency with low-energy data demands a branching fraction well below the LHC reach ( $< 10^{-8}$ ). Constraints on tau rare processes, being less stringent, allow larger  $\tau e$  and  $\tau\mu$  branching ratios [7, 8], hence stimulating these searches at the LHC <sup>1</sup>.

Although these bounds follow from a fairly model-independent analysis (see [8] and references therein), one may also wonder what type of frameworks are capable of producing sizeable lepton flavor violating Higgs decays. Efforts in such direction have been done in different contexts, with pioneer works in Refs. [11, 12]. More recently, Ref. [13] studied the problem in the MSSM, while [14] in the R-parity violating MSSM. Flavor violating decays have been considered as well in the inverse seesaw model in [15]. Possible effects due to vectorlike leptons have been investigated in [16]. Extended scalar sectors involving several Higgs doublets and flavor symmetries (Yukawa textures) have been examined too [17–20] <sup>2</sup>. Finally, the Type-III Two Higgs Doublet Model (2HDM) has been considered in Refs. [24, 25]. Basically, the bottom line of all these analyses is that unless one deals with extra Higgs doublets, lepton flavor violating Higgs decays are below the LHC reach.

In this paper, we study the viability of producing the CMS excess signal in the Type-III 2HDM. For simplicity, we assume flavor violation only in the lepton sector <sup>3</sup> and adopt a pure phenomenological approach, that is to say all the parameters of the model are treated as free parameters subject only to phenomenological constraints. The phenomenological restrictions we consider are the following. First of all, the new degrees of freedom are constrained

\* daristizabal@ulg.ac.be

† avelino.vicente@ulg.ac.be

<sup>1</sup> The impact of lepton flavor violating couplings in the Higgs sector on several low-energy processes was recently studied in [9, 10].

<sup>2</sup> Minimal flavor violating and Froggatt-Nielsen frameworks [21, 22] have been investigated using an effective approach in Ref. [23]. It has been pointed out that in their most simple versions either schemes lead to nonobservable effects.

<sup>3</sup> For flavor violating effects in the quark sector see e.g. Refs. [26, 27].

by electroweak precision data. Thus, in our analysis we calculate the contributions to the  $T$  parameter (contributions to the  $S$  and  $U$  parameters in the 2HDM are small [28]). Since the couplings that induce  $h \rightarrow \tau\mu$  induce as well tau rare processes, we consider the restrictions arising from  $\tau \rightarrow \mu\gamma$  (for which we include Barr-Zee diagrams contributions [29] as done in [24]),  $\tau \rightarrow 3\mu$  and  $\tau \rightarrow \eta\mu$ . We also study whether our scenario can explain the  $(g-2)_\mu$  discrepancy. In contrast to previous studies in the 2HDM, we also verify that the Higgs standard properties deviate only within the allowed measured ranges [3]. These include the following Higgs decay channels:  $\tau\bar{\tau}$ ,  $b\bar{b}$ ,  $WW^*$  and  $ZZ^*$ . We check as well for theoretical constraints, namely that the scalar potential is bounded from below and contains perturbative parameters.

The rest of the paper is organized as follows. In sec. II we discuss basic aspects of the Type-III 2HDM and introduce the formulas employed in our numerical calculation. In sec. III we describe the strategy followed in our numerical analysis and present our results. Finally, in sec. IV we summarize and present our conclusions.

## II. TYPE-III 2HDM

We consider a 2HDM [30, 31] of Type-III. Contrary to other versions of the 2HDM, the Type-III 2HDM does not include any discrete symmetry that serves to distinguish between Higgs doublets. Therefore, both Higgs doublets are allowed to couple to all fermion species.

It is common to present the 2HDM in an arbitrary basis in Higgs space. Instead, following [24], we prefer to introduce the model in the so-called Higgs basis. In this basis, only one Higgs doublet acquires a vacuum expectation value (VEV) and the scalar potential of the model (assuming CP conservation) is given by <sup>4</sup>

$$\begin{aligned} \mathcal{V} = & M_{11}^2 H_1^\dagger H_1 + M_{22}^2 H_2^\dagger H_2 - \left( M_{12}^2 H_1^\dagger H_2 + \text{h.c.} \right) \\ & + \frac{\Lambda_1}{2} \left( H_1^\dagger H_1 \right)^2 + \frac{\Lambda_2}{2} \left( H_2^\dagger H_2 \right)^2 + \Lambda_3 \left( H_1^\dagger H_1 \right) \left( H_2^\dagger H_2 \right) + \Lambda_4 \left( H_1^\dagger H_2 \right) \left( H_2^\dagger H_1 \right) \\ & \left[ \frac{\Lambda_5}{2} \left( H_1^\dagger H_2 \right)^2 + \Lambda_6 \left( H_1^\dagger H_1 \right) \left( H_1^\dagger H_2 \right) + \Lambda_7 \left( H_2^\dagger H_2 \right) \left( H_1^\dagger H_2 \right) + \text{h.c.} \right], \end{aligned} \quad (1)$$

where

$$H_1 = \left( \begin{array}{c} G^+ \\ \frac{1}{\sqrt{2}} (v + \varphi_1^0 + i G^0) \end{array} \right), \quad H_2 = \left( \begin{array}{c} H^+ \\ \frac{1}{\sqrt{2}} (\varphi_2^0 + i A) \end{array} \right), \quad (2)$$

are the Higgs doublets in the Higgs basis, such that  $\langle H_1^0 \rangle = v/\sqrt{2}$  and  $\langle H_2^0 \rangle = 0$ . Here  $\varphi_1^0$  and  $\varphi_2^0$  are CP-even neutral Higgs fields,  $A$  is a CP-odd neutral Higgs field,  $H^+$  is a charged Higgs field and  $G^+$  and  $G^0$  are Goldstone bosons. Since we assume CP conservation,  $A$  is the physical pseudoscalar Higgs and does not mix with  $\varphi_1^0$  and  $\varphi_2^0$ . The relation between  $\varphi_1^0$  and  $\varphi_2^0$  and the scalar mass eigenstates  $h$  and  $H$  (with  $m_h < m_H$ ) is

$$h = \sin(\beta - \alpha) \varphi_1^0 + \cos(\beta - \alpha) \varphi_2^0, \quad (3)$$

$$H = \cos(\beta - \alpha) \varphi_1^0 - \sin(\beta - \alpha) \varphi_2^0. \quad (4)$$

Here we have introduced  $\beta - \alpha$ , the physical mixing angle that relates the Higgs basis and the mass basis for the CP-even scalar states. The potential parameters are related to the physical Higgs masses as

$$m_{H^+}^2 = M_{22}^2 + \frac{v^2}{2} \Lambda_3, \quad (5)$$

$$m_A^2 - m_{H^+}^2 = -\frac{v^2}{2} (\Lambda_5 - \Lambda_4), \quad (6)$$

$$m_H^2 + m_h^2 - m_A^2 = v^2 (\Lambda_1 + \Lambda_5), \quad (7)$$

$$(m_H^2 - m_h^2)^2 = [m_A^2 + (\Lambda_5 - \Lambda_1) v^2]^2 + 4 \Lambda_6^2 v^4, \quad (8)$$

$$\sin[2(\beta - \alpha)] = -\frac{2 \Lambda_6 v^2}{m_H^2 - m_h^2}. \quad (9)$$

---

<sup>4</sup> We follow the conventions of [24, 32] and denote the potential parameters in the Higgs basis in upper case.

We now turn to the Yukawa interactions of the model. In the Higgs basis for the Higgs doublets and the mass basis for the fermions, the Yukawa Lagrangian of the model can be written as

$$\begin{aligned}
-\mathcal{L}_Y = & \sqrt{2} \left( \overline{q_{Lj}} \tilde{H}_1 \frac{K_{ij}^* m_i^U}{v} u_{Ri} + \overline{q_{Li}} H_1 \frac{m_i^D}{v} d_{Ri} + \overline{\ell_{Li}} H_1 \frac{m_i^E}{v} e_{Ri} \right) \\
& + \overline{q_{Li}} \tilde{H}_2 \rho_{ij}^U u_{Rj} + \overline{q_{Li}} H_2 \rho_{ij}^D d_{Rj} + \overline{\ell_{Li}} H_2 \rho_{ij}^E e_{Rj} + \text{h.c.} .
\end{aligned} \tag{10}$$

Here we denote  $\tilde{H}_a = i\sigma_2 H_a^*$ , the fermions ( $u_L, d_L, e_L, u_R, d_R, e_R$ ) are mass eigenstates,  $K$  is the CKM matrix and  $i, j = 1, 2, 3$  are generation indices.  $m_i^U, m_i^D$  and  $m_i^E$  are the up-type quark, down-type quark and charged lepton masses, respectively, and  $\rho^U, \rho^D$  and  $\rho^E$  are general  $3 \times 3$  complex matrices in flavor space. For simplicity, in the following we will assume that the  $\rho$  matrices are hermitian. Now, using Eqs. (2), (3) and (4) we can rewrite the leptonic part of  $\mathcal{L}_Y$  as

$$\begin{aligned}
-\mathcal{L}_Y^{\text{leptons}} = & \bar{e}_i \left( \frac{m_i^E}{v} \delta_{ij} s_{\beta-\alpha} + \frac{1}{\sqrt{2}} \rho_{ij}^E c_{\beta-\alpha} \right) e_j h \\
& + \bar{e}_i \left( \frac{m_i^E}{v} \delta_{ij} c_{\beta-\alpha} - \frac{1}{\sqrt{2}} \rho_{ij}^E s_{\beta-\alpha} \right) e_j H \\
& + \frac{i}{\sqrt{2}} \bar{e}_i \rho_{ij}^E \gamma_5 e_j A + \left[ \bar{\nu}_i (U^\dagger \rho^E)_{ij} P_R e_j H^+ + \text{h.c.} \right],
\end{aligned} \tag{11}$$

where  $U$  is the PMNS matrix,  $P_R = (1 + \gamma_5)/2$  is the usual right-handed chirality projector,  $s_{\beta-\alpha} = \sin(\beta - \alpha)$  and  $c_{\beta-\alpha} = \cos(\beta - \alpha)$ . From Eq. (11) we can extract the Higgs couplings to fermions

$$g_{hff'} = \frac{m_f}{v} s_{\beta-\alpha} \delta_{ff'} + \frac{\rho_{ff'}}{\sqrt{2}} c_{\beta-\alpha}, \tag{12}$$

$$g_{Hff'} = \frac{m_f}{v} c_{\beta-\alpha} \delta_{ff'} - \frac{\rho_{ff'}}{\sqrt{2}} s_{\beta-\alpha}, \tag{13}$$

$$g_{Aff'} = \pm i \gamma_5 \frac{\rho_{ff'}}{\sqrt{2}}, \tag{14}$$

where  $g_{Aff'} = +i\gamma_5 \frac{\rho_{ff'}}{\sqrt{2}}$  for down-type quarks and charged leptons and  $g_{Aff'} = -i\gamma_5 \frac{\rho_{ff'}}{\sqrt{2}}$  for up-type quarks. Finally, we will consider a specific structure for the  $\rho$  matrices inspired in the *Cheng-Sher ansatz* [33]. First, we normalize  $\rho^E$  as

$$\rho_{ij}^E = -\kappa_{ij} \tan \beta_\tau \sqrt{\frac{2m_i m_j}{v^2}}, \tag{15}$$

where  $m_i \equiv m_i^E$  and  $\beta_\tau$  is the physical mixing angle defined by the ratio <sup>5</sup>

$$\tan \beta_\tau = \frac{-\rho_{\tau\tau}}{\sqrt{2}m_\tau/v}. \tag{16}$$

Note that, by definition,  $\kappa_{\tau\tau} = 1$ . However, the other  $\kappa_{ij}$ 's, and in particular,  $\kappa_{\tau\mu} = \kappa_{\mu\tau}^*$ , are free parameters. For the quark  $\rho$  matrices we assume the following Type-II values

$$\rho_{ij}^D = -\sqrt{2} \tan \beta_\tau \frac{m_i^D}{v} \delta_{ij} \quad , \quad \rho_{ij}^U = \sqrt{2} \cot \beta_\tau \frac{(K^\dagger m^U)_i}{v} \delta_{ij}. \tag{17}$$

This parameterization of the  $\rho$  matrices is not the most general one but, as we will see, it leads to results in good agreement with the experimental constraints. Furthermore, this ansatz can be understood as a minimal correction beyond the Type-II 2HDM, with the only departure in the  $\tau\mu$  coupling [34].

Finally, the Higgs couplings to gauge bosons are fully dictated by the gauge symmetry. One has  $C_{hWW} = s_{\beta-\alpha} C_{hWW}^{\text{SM}}$ ,  $C_{HWW} = c_{\beta-\alpha} C_{hWW}^{\text{SM}}$  and  $C_{AWW} = 0$ . The couplings to a pair of  $Z$ -bosons follow the same proportionality.

<sup>5</sup> In the Type-III 2HDM there is no unique definition of  $\tan \beta$  since one can always apply rotations in Higgs space, acting also on the Higgs VEVs,  $v_1$  and  $v_2$ . Therefore, a specific (physical) definition is required [32]. Since we are interested in tau flavor violation, we choose to define  $\tan \beta_\tau$  as the relative size of the tau Yukawa coupling and  $\sqrt{2}m_\tau/v$ , in analogy to the usual definition of  $\tan \beta$  in the Type-II 2HDM.

### III. PHENOMENOLOGICAL ANALYSIS

We now proceed to describe our phenomenological analysis. Our results are based on a random scan of the parameter space, with the following ranges for the relevant input parameters:

$$m_H \in [200, 1000] \text{ GeV}, \quad m_A \in [400, 1000] \text{ GeV}, \quad (18)$$

$$m_{H^\pm} = m_A + \delta m, \quad \text{with} \quad \delta m \in [-5, 5] \text{ GeV}, \quad (19)$$

$$\sin(\beta - \alpha) \in [0.7, 1.0], \quad \tan \beta_\tau \in [0.1, 40], \quad (20)$$

$$|\kappa_{\tau\mu}| \in [0.1, 3]. \quad (21)$$

In addition, we assume  $m_h = 126$  GeV. Since we are driven by phenomenological considerations, we use as input the scalar masses ( $m_h$ ,  $m_H$ ,  $m_A$  and  $m_{H^\pm}$ ) rather than the parameters in the scalar potential. Our choice of a small mass difference between the pseudoscalar and charged Higgses is motivated by the reduction of the  $T$  parameter<sup>6</sup>, whereas the lower limits on  $\sin(\beta - \alpha)$  and  $m_{H^\pm}$  (as induced by the lower limit on  $m_A$ ) are motivated by experimental constraints: smaller values of  $\sin(\beta - \alpha)$  would be excluded by current measurements of the Higgs couplings to fermions and gauge bosons while lower  $m_{H^\pm}$  would lead to certain tension with flavor physics bounds (mainly B physics, see [27] for a review). We emphasize that the mass ranges selected for our numerical scan are quite conservative since lower values for  $m_H$ ,  $m_A$  and  $m_{H^\pm}$  are allowed by LHC data, see e.g. [35].

After choosing input parameters three checks are performed:

- We determine  $\Lambda_1$ ,  $\Lambda_4$ ,  $\Lambda_5$  and  $\Lambda_6$  by means of Eqs. (5)-(9) and only allow those parameter points where the resulting values are below  $4\pi$ . The exact value of this perturbativity constraint is somehow arbitrary (see for example the discussion in [37–39]). However, we have checked that it has no impact on our numerical results<sup>7</sup>. Furthermore, we also ensure boundedness from below [37, 41, 42] by properly choosing the remaining  $\Lambda$  parameters.
- We explicitly compute the  $T$  parameter and discard parameter points outside the current  $1\sigma$  region, given by  $T \in [-0.03, 0.19]$  [43].
- Finally, we check whether the Higgs couplings agree with the current CMS measurements [3]. More precisely, we determine the signal strengths for  $h \rightarrow \tau\bar{\tau}, b\bar{b}, WW^*, ZZ^*$ , defined as  $\mu = (\sigma \times \text{BR}) / (\sigma \times \text{BR})_{\text{SM}}$ , and compare them to the CMS  $1\sigma$  ranges [3]. We assume that Higgs production is given by gluon fusion (neglecting other production mechanisms, a fairly good approximation) and compute the signal strengths as

$$\mu_{XX} = \left( \frac{g_{htt}}{g_{htt}^{\text{SM}}} \right)^2 \left( \frac{g_{hXX}}{g_{hXX}^{\text{SM}}} \right)^2. \quad (22)$$

Here  $g_{htt}$  and  $g_{hXX}$  are the Higgs boson couplings to a pair of top quarks and  $X \equiv \tau, b, W, Z$ , respectively. The superscript SM indicates standard model values.

These constraints impose severe restrictions on the allowed parameter space of the model (most parameter points are actually excluded) and their consideration is required to properly address the Type-III 2HDM as responsible for the CMS  $h \rightarrow \tau\mu$  signal excess. After these checks are passed, the observables are computed using the analytical expressions of [24]. In particular, we compute the branching ratio for  $h \rightarrow \tau\mu$  as

$$\text{BR}(h \rightarrow \tau\mu) = \frac{m_h}{8\pi\Gamma_h} (|g_{h\tau\mu}|^2 + |g_{h\mu\tau}|^2), \quad (23)$$

where  $\Gamma_h$  is the Higgs boson total decay width<sup>8</sup>. For the analytical expressions required for the computation of  $\text{BR}(\tau \rightarrow \mu\gamma)$  we refer the reader to Appendix A.

Fig. 1 shows our results for  $\text{BR}(h \rightarrow \tau\mu)$  as a function of  $\text{BR}(\tau \rightarrow \mu\gamma)$ . The horizontal lines define the  $1\sigma$  interval around the observed  $\text{BR}(h \rightarrow \tau\mu)$  at CMS [6]. The vertical lines show the current experimental limit set by BaBar,  $\text{BR}(\tau \rightarrow \mu\gamma) < 4.4 \times 10^{-8}$  [44], and an expected sensitivity at Belle-II of about  $\sim 10^{-9}$  [45]. As can be clearly seen, there is a correlation between  $\text{BR}(h \rightarrow \tau\mu)$  and  $\text{BR}(\tau \rightarrow \mu\gamma)$ . However, cancellations among the different contributions to  $\text{BR}(\tau \rightarrow \mu\gamma)$  preclude any definitive prediction for this observable. We find that the dominant

<sup>6</sup> An alternative choice is given by  $m_{H^\pm} = m_{H^0} + \delta m$ , see [36] for details.

<sup>7</sup> We point out that a more rigorous check based on tree-level unitarity was introduced in [40].

<sup>8</sup> Given the constraints on the Higgs boson couplings, the computed  $\Gamma_h$  turns out to be close to the SM value,  $\Gamma_h^{\text{SM}} \simeq 4.1$  MeV.

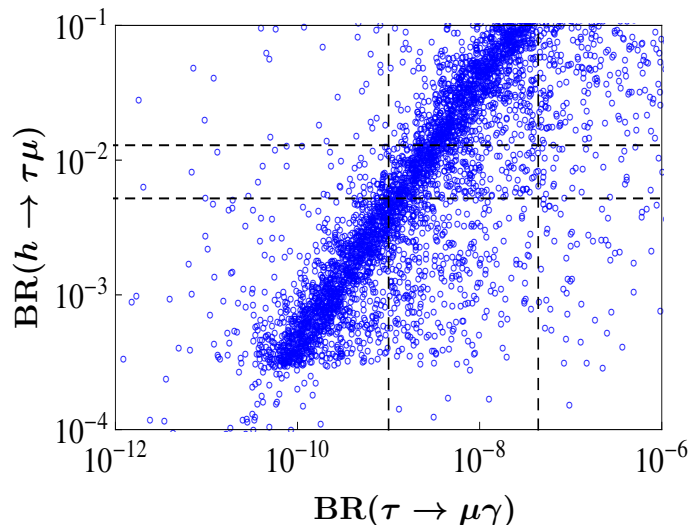


FIG. 1.  $\text{BR}(h \rightarrow \tau\mu)$  as a function of  $\text{BR}(\tau \rightarrow \mu\gamma)$  for the relevant parameters fixed according to Eqs. (18)-(21). The horizontal lines show the  $1\sigma$  interval around the best-fit value for  $\text{BR}(h \rightarrow \tau\mu)$ , as observed by CMS [6]. The right vertical line corresponds to the current experimental limit  $\text{BR}(\tau \rightarrow \mu\gamma) < 4.4 \times 10^{-8}$  [44], whereas the left vertical line represents an expected sensitivity at Belle-II of about  $\sim 10^{-9}$  [45].

contribution is typically given by 2-loop Barr-Zee diagrams [29, 46] with internal  $W$  bosons, although the other contributions considered in our numerical evaluation<sup>9</sup> may have similar sizes (and even become dominant in some cases). We conclude that it is possible to explain the CMS excess in  $h \rightarrow \tau\mu$ , while being compatible with the current bound on  $\text{BR}(\tau \rightarrow \mu\gamma)$  as well as the abovementioned constraints on the scalar potential, the Higgs couplings and the  $T$  parameter. This is the main result of this paper.

Regarding the required values for the model parameters, a sizable  $\kappa_{\tau\mu} \sim 0.5 - 0.8$  is necessary. This is the key parameter in the determination of  $\text{BR}(h \rightarrow \tau\mu)$ . In contrast, we find little dependence with the other parameters (when taken individually), although specific ranges are favored by the experimental constraints. In what concerns  $\tan\beta_\tau$ , a value  $\tan\beta_\tau \gtrsim 2$  is necessary to be compatible with the constraints on the Higgs boson couplings. The  $\beta - \alpha$  angle should depart from  $\pi/2$  (which would correspond to the decoupling limit) and have values in the  $\sin(\beta - \alpha) \sim 0.9$  ballpark. Finally, we find a preference for large  $\Lambda$  parameters, required to generate a hierarchy in the scalar spectrum.

In Fig. 2 we present our results for the allowed signal strengths in the  $b\bar{b}$ ,  $WW^*$  and  $ZZ^*$  channels<sup>10</sup>. As usual, they are normalized to their SM values and thus the vertical line at  $\mu_{XX} = 1$  represents the SM prediction. The purple bars cover the complete  $1\sigma$  ranges compatible with measurements by CMS [3], with the black dots at the best-fit values. The orange bars represent the allowed signal strengths in the Type-III 2HDM as required to obtain  $\text{BR}(h \rightarrow \tau\mu) = (0.89^{+0.40}_{-0.37})\%$ . We do not show the results for the  $\tau\tau$  channel because they do not provide any information, as the purple and orange bars extend over the same range. The most interesting results are those for the  $WW^*$  and  $ZZ^*$  channels,  $\mu_{WW}, \mu_{ZZ} \in [0.71, 0.99]$ . For both, a measurement implying  $\mu > 1$  would rule out our scenario. In contrast, for the  $b\bar{b}$  channel both  $\mu_{bb} < 1$  and  $\mu_{bb} > 1$  are compatible with the CMS measurement of  $\text{BR}(h \rightarrow \tau\mu)$ , although the allowed bar shrinks to a narrower range,  $\mu_{bb} \in [0.64, 1.18]$ . Nevertheless, we note that the results for this channel are related to the ansatz assumed in Eq. (17).

Finally, we have also considered the LFV processes  $\tau \rightarrow \eta\mu$  and  $\tau \rightarrow 3\mu$ . However, we have found that the constraints on the model derived from their experimental bounds are weaker than those obtained from the radiative  $\tau \rightarrow \mu\gamma$ . Furthermore, our numerical results show that the  $(g-2)_\mu$  anomaly cannot be explained within our scenario, in agreement with [24].

<sup>9</sup> Following [47], these are 1-loop diagrams with a Higgs boson in the loop and 2-loop Barr-Zee diagrams with internal t- and b-quarks, see Appendix A.

<sup>10</sup> A recent global fit of the Higgs couplings in the Type-I and Type-II 2HDM was presented in [48].

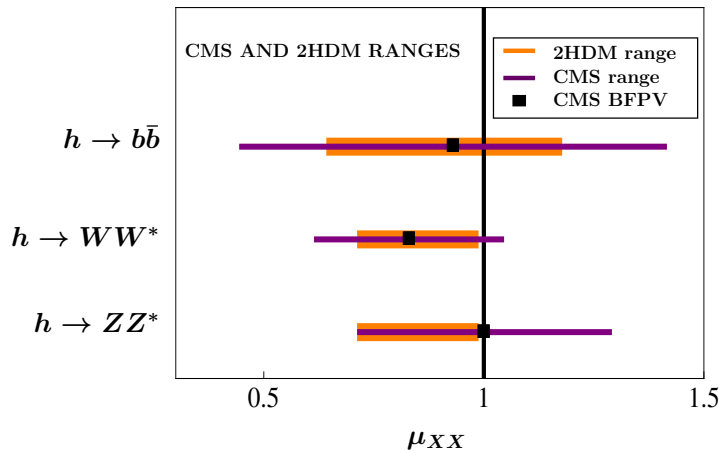


FIG. 2. Allowed signal strengths in the Type-III 2HDM as required to produce  $\text{BR}(h \rightarrow \tau\mu)$  in agreement with the signal found at CMS (within  $1\sigma$ ) while at the time satisfying electroweak precision data ( $T$  parameter constraints) as well as low-energy data. The purple (thin) bars cover the  $1\sigma$  uncertainties obtained by CMS (with the black dots at the best-fit values), whereas the orange (thick) bars represent the allowed signal strengths in the Type-III 2HDM as required to obtain  $\text{BR}(h \rightarrow \tau\mu) = (0.89^{+0.40}_{-0.37})\%$ .

#### IV. CONCLUSIONS

The excess of signal events in the  $\tau\mu$  Higgs boson decay channel reported by the CMS collaboration poses a challenge for beyond SM physics models. Basically, apart from models involving extra Higgs doublets, no models capable of producing Higgs lepton flavor violating measurable at LHC have been put forward. Certainly, the 2HDM is the simplest of such extensions, and in its Type-III “incarnation” combines the elements that—in principle—can yield an explanation to CMS data.

Driven by this motivation, in this paper, we have done a detailed study of the Type-III 2HDM. In our analysis, we have paid special attention to all relevant constraints, which include: (i) boundedness from below and perturbativity of the scalar potential; (ii) electroweak precision data; (iii) low-energy  $\tau$  lepton flavor violating decay constraints; (iv) standard Higgs decay channels. Our findings show that generating a large  $h \rightarrow \tau\mu$  branching fraction, as required by CMS data, turns out to be possible while satisfying criteria (i)-(iv). Conditions in (i) do not lead to significant constraints due to large parameter freedom. Conditions in (ii) and (iii) do not represent either any unavoidable restriction. We have found that the most stringent constraints arise from requiring the Higgs boson to obey current limits on its standard decay channels:  $b\bar{b}$ ,  $\tau\bar{\tau}$ ,  $WW^*$ ,  $ZZ^*$ , although never threatening the production of the CMS signal.

In summary, in this paper we have demonstrated that the Type-III 2HDM with a *Cheng-Sher ansatz*-inspired flavor structure naturally accounts for the CMS excess signal. Of course, if this excess persist pinning down its origin will require an extensive experimental effort. However, we stress that it might be the first indication of a more complex scalar structure. Moreover, since *Cheng-Sher* flavor structures emerge from flavor symmetries, these data might even reveal the presence of a fundamental flavor symmetry [49].

#### ACKNOWLEDGEMENTS

DAS and AV want to thank Martin Hirsch for drawing their attention to the CMS results and Sacha Davidson for the illuminating and inspiring conversations that led to this work, for her suggestions, encouragement and comments on the manuscript. AV is grateful to Alejandro Celis for fruitful discussions on the subject of Higgs lepton flavor violation in the 2HDM. We would like to thank as well Ben O’Leary and Igor Ivanov for comments. DAS would like to acknowledge financial support from the Belgian FNRS agency through a “Chargé de Recherche” contract. AV acknowledges partial support from the EXPL/FIS-NUC/0460/2013 project financed by the Portuguese FCT.

### Appendix A: Analytical expressions for $\tau \rightarrow \mu\gamma$

In this appendix we give the required analytical expressions for the computation of the  $\tau \rightarrow \mu\gamma$  rate. This radiative process is induced by the dipole operator

$$C^{ij}\bar{e}_i\sigma^{\alpha\beta}P_R e_j F_{\alpha\beta} + \text{h.c.}, \quad (\text{A1})$$

where  $i, j$  are the flavors of the external leptons,  $F_{\alpha\beta}$  is the electromagnetic strength tensor and  $\sigma^{\alpha\beta} = \frac{i}{2} [\gamma^\alpha, \gamma^\beta]$ . The coefficients  $C^{ij}$  can be related to the form factors  $A_L$  and  $A_R$ ,

$$C^{\tau\mu} = \frac{e m_\tau A_R^{\tau\mu}}{2}, \quad C^{\mu\tau*} = \frac{e m_\tau A_L^{\tau\mu}}{2}, \quad (\text{A2})$$

which appear in the  $\tau \rightarrow \mu\gamma$  branching ratio as

$$\text{BR}(\tau \rightarrow \mu\gamma) = \text{BR}(\tau \rightarrow \mu\nu\bar{\nu}) \frac{48\pi^3\alpha}{G_F^2} (|A_L|^2 + |A_R|^2). \quad (\text{A3})$$

In the model under consideration  $|g_{h\tau\mu}| = |g_{h\mu\tau}|$ , which leads to  $|A_L| = |A_R| \equiv |A|$ . As in [24], we will consider three contributions to the form factor  $A$ : 1-loop diagrams with neutral Higgs bosons and charged leptons in the loop, 2-loop Barr-Zee diagrams with an internal photon and a third generation quark, and 2-loop Barr-Zee diagrams with an internal photon and a  $W$ -boson [47]. Therefore, we write

$$A = \frac{1}{16\pi^2} (A_1 + A_2^{t,b} + A_2^W). \quad (\text{A4})$$

The different contributions are [24]

$$A_1 = \sqrt{2} \sum_\phi \frac{g_{\phi\mu\tau} g_{\phi\tau\tau}}{m_\phi^2} \left( \ln \frac{m_\phi^2}{m_\tau^2} - \frac{3}{2} \right), \quad (\text{A5})$$

$$A_2^{t,b} = 2 \sum_{\phi,f} g_{\phi\mu\tau} g_{\phi ff} \frac{N_c Q_f^2 \alpha}{\pi} \frac{1}{m_\tau m_f} f_\phi \left( \frac{m_f^2}{m_\phi^2} \right), \quad (\text{A6})$$

$$A_2^W = - \sum_{\phi=h,H} g_{\phi\mu\tau} C_{\phi WW} \frac{g\alpha}{2\pi m_\tau m_W} \left[ 3f_\phi \left( \frac{m_W^2}{m_\phi^2} \right) + \frac{23}{4} g \left( \frac{m_W^2}{m_\phi^2} \right) + \frac{3}{4} h \left( \frac{m_W^2}{m_\phi^2} \right) + m_\phi^2 \frac{f_\phi \left( \frac{m_W^2}{m_\phi^2} \right) - g \left( \frac{m_W^2}{m_\phi^2} \right)}{2m_W^2} \right]. \quad (\text{A7})$$

Here  $\phi = h, H, A$ ,  $f = t, b$ , the coupling  $g_{\phi ff'}$  of the internal loop fermion to the  $\phi$  scalar is given in Eqs. (12)-(14) and the couplings  $C_{\phi WW}$  are given in the last paragraph of Sec. II. In Eqs. (A5)-(A7) lepton masses have been neglected whenever possible. Finally, the loop functions in the previous expressions are [47]

$$f_A(z) \equiv g(z) = \frac{z}{2} \int_0^1 dx \frac{1}{x(1-x)-z} \ln \frac{x(1-x)}{z}, \quad (\text{A8})$$

$$f_{h,H}(z) = \frac{z}{2} \int_0^1 dx \frac{(1-2x(1-x))}{x(1-x)-z} \ln \frac{x(1-x)}{z}, \quad (\text{A9})$$

$$h(z) = -\frac{z}{2} \int_0^1 \frac{dx}{x(1-x)-z} \left[ 1 - \frac{z}{x(1-x)-z} \ln \frac{x(1-x)}{z} \right]. \quad (\text{A10})$$



- 
- [1] S. Chatrchyan *et al.* [CMS Collaboration], Phys. Lett. B **716**, 30 (2012) [arXiv:1207.7235 [hep-ex]].
- [2] G. Aad *et al.* [ATLAS Collaboration], Phys. Lett. B **716**, 1 (2012) [arXiv:1207.7214 [hep-ex]].
- [3] CMS Collaboration, “Precise determination of the mass of the Higgs boson and studies of the compatibility of its couplings with the standard model”, *CMS Physics Analysis Summary* CMS-PAS-HIG-14-009 (2014)
- [4] G. Aad *et al.* [ATLAS Collaboration], Phys. Rev. Lett. **112**, 201802 (2014) [arXiv:1402.3244 [hep-ex]].
- [5] S. Chatrchyan *et al.* [CMS Collaboration], Eur. Phys. J. C **74**, 2980 (2014) [arXiv:1404.1344 [hep-ex]].
- [6] CMS Collaboration, “Search for lepton flavor violating decays of the Higgs boson”, *CMS Physics Analysis Summary* CMS-PAS-HIG-14-005 (2014).
- [7] G. Blankenburg, J. Ellis and G. Isidori, Phys. Lett. B **712**, 386 (2012) [arXiv:1202.5704 [hep-ph]].
- [8] R. Harnik, J. Kopp and J. Zupan, JHEP **1303**, 026 (2013) [arXiv:1209.1397 [hep-ph]].
- [9] A. Goudelis, O. Lebedev and J. h. Park, Phys. Lett. B **707** (2012) 369 [arXiv:1111.1715 [hep-ph]].
- [10] A. Celis, V. Cirigliano and E. Passemar, Phys. Rev. D **89** (2014) 013008 [arXiv:1309.3564 [hep-ph]].
- [11] A. Pilaftsis, Phys. Lett. B **285** (1992) 68.
- [12] J. L. Diaz-Cruz and J. J. Toscano, Phys. Rev. D **62** (2000) 116005 [hep-ph/9910233].
- [13] M. Arana-Catania, E. Arganda and M. J. Herrero, JHEP **1309**, 160 (2013) [arXiv:1304.3371 [hep-ph]].
- [14] A. Arhrib, Y. Cheng and O. C. W. Kong, Europhys. Lett. **101**, 31003 (2013) [arXiv:1208.4669 [hep-ph]].
- [15] E. Arganda, M. J. Herrero, X. Marcano and C. Weiland, arXiv:1405.4300 [hep-ph].
- [16] A. Falkowski, D. M. Straub and A. Vicente, JHEP **1405**, 092 (2014) [arXiv:1312.5329 [hep-ph]].
- [17] G. Bhattacharyya, P. Leser and H. Päs, Phys. Rev. D **83**, 011701 (2011) [arXiv:1006.5597 [hep-ph]].
- [18] G. Bhattacharyya, P. Leser and H. Päs, Phys. Rev. D **86**, 036009 (2012) [arXiv:1206.4202 [hep-ph]].
- [19] M. Arroyo, J. L. Diaz-Cruz, E. Diaz and J. A. Orduz-Ducua, arXiv:1306.2343 [hep-ph].
- [20] M. D. Campos, A. E. C. Hernández, H. Päs and E. Schumacher, arXiv:1408.1652 [hep-ph].
- [21] G. D’Ambrosio, G. F. Giudice, G. Isidori and A. Strumia, Nucl. Phys. B **645**, 155 (2002) [hep-ph/0207036].
- [22] C. D. Froggatt and H. B. Nielsen, Nucl. Phys. B **147**, 277 (1979).
- [23] A. Dery, A. Efrati, Y. Nir, Y. Soreq and V. Susič, arXiv:1408.1371 [hep-ph].
- [24] S. Davidson and G. J. Grenier, Phys. Rev. D **81**, 095016 (2010) [arXiv:1001.0434 [hep-ph]].
- [25] J. Kopp and M. Nardecchia, arXiv:1406.5303 [hep-ph].
- [26] D. Atwood, L. Reina and A. Soni, Phys. Rev. D **55**, 3156 (1997) [hep-ph/9609279].
- [27] A. Crivellin, A. Kokulu and C. Greub, Phys. Rev. D **87** (2013) 9, 094031 [arXiv:1303.5877 [hep-ph]].
- [28] D. O’Neil, arXiv:0908.1363 [hep-ph].
- [29] S. M. Barr and A. Zee, Phys. Rev. Lett. **65** (1990) 21 [Erratum-ibid. **65** (1990) 2920].
- [30] T. D. Lee, Phys. Rev. D **8** (1973) 1226.
- [31] G. C. Branco, Phys. Rev. D **22** (1980) 2901.
- [32] S. Davidson and H. E. Haber, Phys. Rev. D **72** (2005) 035004 [Erratum-ibid. D **72** (2005) 099902] [hep-ph/0504050].
- [33] T. P. Cheng and M. Sher, Phys. Rev. D **35** (1987) 3484.
- [34] S. Kanemura, T. Ota and K. Tsumura, Phys. Rev. D **73** (2006) 016006 [hep-ph/0505191].
- [35] A. Celis, V. Ilisie and A. Pich, JHEP **1312** (2013) 095 [arXiv:1310.7941 [hep-ph]].
- [36] J.-M. Gerard and M. Herquet, Phys. Rev. Lett. **98**, 251802 (2007) [hep-ph/0703051 [HEP-PH]].
- [37] P. M. Ferreira and D. R. T. Jones, JHEP **0908** (2009) 069 [arXiv:0903.2856 [hep-ph]].
- [38] D. Eriksson, J. Rathsmann and O. Stal, Comput. Phys. Commun. **181** (2010) 189 [arXiv:0902.0851 [hep-ph]].
- [39] A. Broggio, E. J. Chun, M. Passera, K. M. Patel and S. K. Vempati, arXiv:1409.3199 [hep-ph].
- [40] I. F. Ginzburg and I. P. Ivanov, Phys. Rev. D **72** (2005) 115010 [hep-ph/0508020].
- [41] I. P. Ivanov, Phys. Rev. D **75** (2007) 035001 [Erratum-ibid. D **76** (2007) 039902] [hep-ph/0609018].
- [42] I. P. Ivanov, Phys. Rev. D **77** (2008) 015017 [arXiv:0710.3490 [hep-ph]].
- [43] M. Baak, M. Goebel, J. Haller, A. Hoecker, D. Kennedy, R. Kogler, K. Moenig and M. Schott *et al.*, Eur. Phys. J. C **72** (2012) 2205 [arXiv:1209.2716 [hep-ph]].
- [44] B. Aubert *et al.* [BaBar Collaboration], Phys. Rev. Lett. **104** (2010) 021802 [arXiv:0908.2381 [hep-ex]].
- [45] T. Aushev, W. Bartel, A. Bondar, J. Brodzicka, T. E. Browder, P. Chang, Y. Chao and K. F. Chen *et al.*, arXiv:1002.5012 [hep-ex].
- [46] J. D. Bjorken, K. D. Lane and S. Weinberg, Phys. Rev. D **16** (1977) 1474.
- [47] D. Chang, W. S. Hou and W. Y. Keung, Phys. Rev. D **48** (1993) 217 [hep-ph/9302267].
- [48] J. Bernon, B. Dumont and S. Kraml, arXiv:1409.1588 [hep-ph].
- [49] A. Antaramian, L. J. Hall and A. Rasin, Phys. Rev. Lett. **69** (1992) 1871 [hep-ph/9206205].